Original Article

MEMOIRS HEALTH SCI. MED. KANAZAWA UNIV. Vol. 22
1～10 1998

Development of New Analysis on ECG Gated SPECT Images (Functional G-Maps Method) : Study in Normal Subjects

Masahisa Onoguchi Hirotaka Maruno*
Teruhiko Takayama Hajime Murata**

ABSTRACT

We developed new analysis (Functional G-maps method) on ECG gated SPECT to evaluate precisely the regional cardiac function and studied in 14 patients with less likelihood of coronary artery disease. Following the first pass method immediately after intravenous injection of 1110 MBq of ^{99m}Tc-tetrofosmin, ECG gated SPECT data were acquired one hour after injection by dividing a cardiac cycle into 12 frames. Firstly every short-axis images were reconstructed from 11 of 12 frames. Furthermore, the reconstruction of these images was repeated after performing slice thickness correction. Excluding the effect of different apex-base length in any frame during a cardiac cycle, 10 short-axis images consisted of the same slice thickness were obtained from each frame. Subsequently each short-axis image was divided by 40 radii into 40 segments. The time activity curve was generated from the total counts included in each segment plus both neighboring segments. Afterwards the curve fitting was performed using the second inverse fourier function. From fitted curves and their differentials, we calculated following parameters ; Max (End-systolic count), Min (End-diastolic count), %CI (Percent count increase), Uptake, PCR (Peak contraction rate), PDR (Peak distention rate) and CT (Contraction time). The %Max was greater in the anterior (96.2%) and septal regions (96.8%), whereas the %Min was greater in the apex (93.6%) and lateral regions (96.9%). The %CI and %PCR were also greater in the septal (101.8%, 4.17%), anterior (98.4%, 3.99%) and inferior regions (94.9%, 3.88%). On the other hand, the %PDR in the apex (3.58%) and lateral (3.23%) regions were lower than the values in the other regions, but the significant difference was not shown among each region. The CT was greater in the apex (110.5%) and lateral regions (110.5%). Consequently, functional G-maps demonstrated clearly regional cardiac function. In conclusion, this method is expected to be helpful for accurate assessment of cardiac function.

KEY WORDS

ECG gated SPECT, Cardiac functional analysis, Tc-99m-tetrofosmin, Functional G-maps

INTRODUCTION

Myocardial scintigraphy with technetium-99m tetrofosmin (tetrofosmin) or sestamibi (MIBI)[1)-3)] has been used in evaluating myocardial perfusion in patients with coronary artery diseases (CAD). Most of such patients reveal so

Department of Radiological Technology, School of Health Sciences, Faculty of Medicine, Kanazawa University
* Division of Nuclear Medicine, Toranomon Hospital, Tokyo
** National Institute of Radiological Sciences, Chiba

impaired cardiac function that it is important to evaluate cardiac function. If it is possible to evaluate simultaneously cardiac function as well as myocardial perfusion by single injection of tracer[4)-6)], it is preferable from the viewpoint of convenience and cost performance. Electrocardiographic (ECG) gated data acquisition in single photon emission computed tomography (SPECT) provides the potential for simultaneous assessment of them. However, the achievement requires so much time in data acquisition and processing that routine use of protocols is restricted in the institution where a supercomputer and/or multi-detector SPECT system were equipped with. Since the first report by Moore et al.[6)] in 1980 on ECG gated SPECT in cardiac blood pool scintigraphy, a variety of parameters have been defined to estimate left ventricular function. They include left ventricular ejection fraction (LVEF), amplitude, phase, percent count increase (%CI) and percent wall thickening (%WT)[7)-12)]. Many authors estimated these parameters by the value and/or the curve pattern, and the concept of functional images is not so much reported[7)-8), 12)]

The aim of this study was to develop new analysis on ECG gated SPECT that can represent new parameters by colored-display on polar map which makes it possible to interpret cardiac function visually, and to assess the values of parameters in normal subjects.

MATERIALS AND METHODS

Study Population

The study population consisted of 14 patients (10 males and 4 females) with less likelihood of coronary artery disease. Their ages ranged from 24 to 61 years (mean age : 40.6±13.7 years). All patients underwent echocardiography, first-pass radionuclide angiography and ECG gated SPECT. Their ECGs showed regular sinus rhythm.

Preparation of ^{99m}Tc-tetrofosmin

^{99m}Tc-tetrofosmin (Nihon Medi-Physics Corp., Tokyo) was prepared from a freeze-dried kit by reconstitution with approximately 2ml of a sterile pertechnetate solution containing 740-1110 MBq of Tc-99m.

Imaging protocol

At fasting and resting, SPECT was imaged one hour after injection of ^{99m}Tc-tetrofosmin using a rotating gamma camera (GE Starcam 4000 XC/T-Star system) equipped with a low energy all-purpose collimator. The energy discrimination was centered on 140keV with a 20% window. Thirty-two projections (50 seconds per projection) were acquired by dividing a cardiac cycle into 12 frames over a 180°, semicircular arc extending from the 45° right anterior oblique (RAO) to the 45° left posterior oblique (LPO) position. All images were obtained with a 64 x 64 matrix and a zoom of 1.33. Twelve frames per cardiac cycle were acquired at each projection. All data acquisition were prefiltered with a Hanning filter (cut off 0.8). The SPECT images were reconstructed using a filtered backprojection algorithm and Ramp filter (cutoff 0). Three kinds of SPECT images were generated : (a) horizontal long axis, (b) vertical long axis, and (c) short axis image. No attenuation correction was performed.

Procedure for Functional G-maps

Expand processing for slices

Figure 1 shows the alignment of short-axis images from the apex to base for each frame during a cardiac cycle. Each image was reconstructed from 11 of 12 frames as usual and the last frame was abandoned. Subsequently the reconstruction of these images was repeated after performing slice thickness correction. Excluding the effect of different apex-base length in any frame during a cardiac cycle, 10 short-axis images consisted of the same slice thickness were obtained from each frame (Fig. 2). To detect automatically the apex and base of short-axis images on each frame, the apex and base in the end-systolic (ES) and the end-diastolic (ED) image were manually found

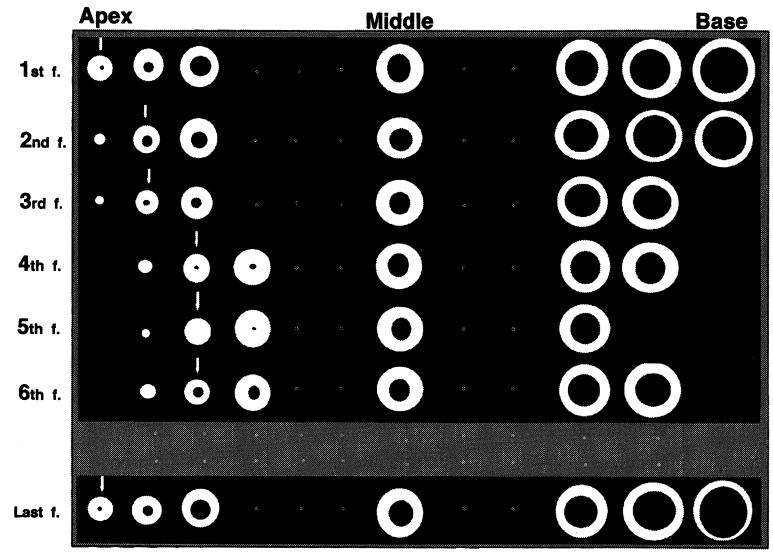

Fig. 1 The alignment of short-axis images from the apex to base for each frame during a cardiac cycle.

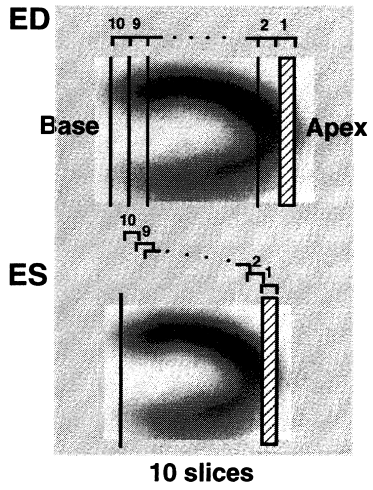

Fig. 2 Technique for slice thickness correction. Apex to-base length at any frame is divided into10 slices with the same thickness.

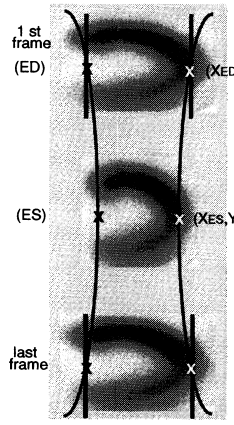

$$Y=A \times \cos(X+B) + d \quad \text{——— (1)}$$

$$A=\frac{Y_{ED} - d}{\cos(X_{ED} + B)} \quad \text{——— (2)}$$

$$\tan(B)=\frac{Y_{ED} \times \cos(X_{ES}) - Y_{ES} \times \cos(X_{ED})}{Y_{ED} \times \sin(X_{ES}) - Y_{ES} \times \sin(X_{ED})} \quad \text{— (3)}$$

$$d=\frac{Y_{ED} + Y_{ES}}{2} \quad \text{——— (4)}$$

Fig. 3 Following the decision of the apex and the base in the coordinate at both the end-diastole and the end-systole by manual, their locations at any frame are automatically determined using the function ; Y=A x cos(X+B)+d.

respectively. On the basis of these locations, the apex and base were automatically determined in each frame. Because the locations of apex and base in the other frames can be approximated by trigonometric function using the least square method, the following formulas can be obtained (Fig. 3)

$$Y=A \times \cos (X + B) + d \quad \text{Eq. 1}$$

$$A= (Y_{ED} - d) / \cos (X_{ED} + B) \quad \text{Eq. 2}$$

$$\tan(B)=[Y_{ED} \times \cos(X_{ES})-Y_{ES} \times \cos(X_{ED})]/ [Y_{ED} \times \sin(X_{ES})-Y_{ES} \times \sin(X_{ED})] \quad \text{Eq. 3}$$

$$d= (Y_{ED} + Y_{ES}) / 2 \quad \text{Eq. 4}$$

where X and Y are the locations of apex and base in any frame respectively and suffix of ES or ED shows the end-systolic (ES) or the end-diastolic (ED) image respectively.

Slice Reframe processing

The short-axis images were aligned after being recontructed with slice thickness correction and images in any frame were reframed with 10 slices (Fig. 4).

Generation of time activity curve

The centers and the radii on the apical and

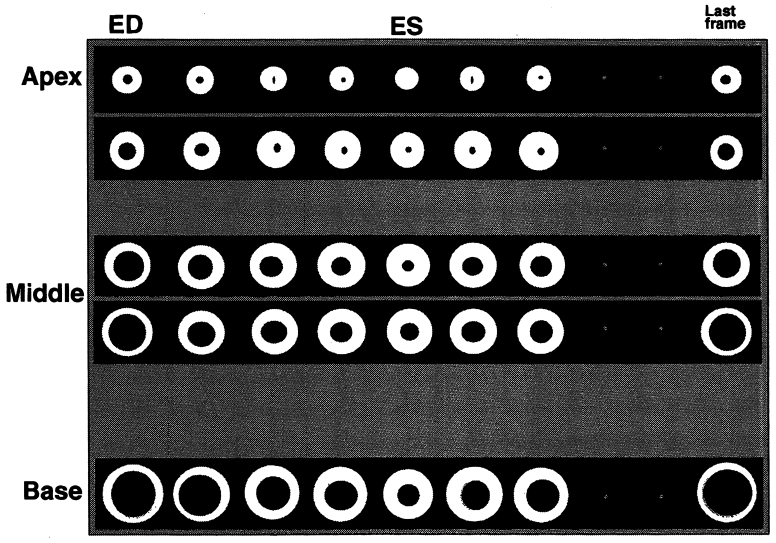

Fig. 4 The alignment of short-axis images after the recontruction with slice thickness correction. Images at any frame are reframed with 10 slices.

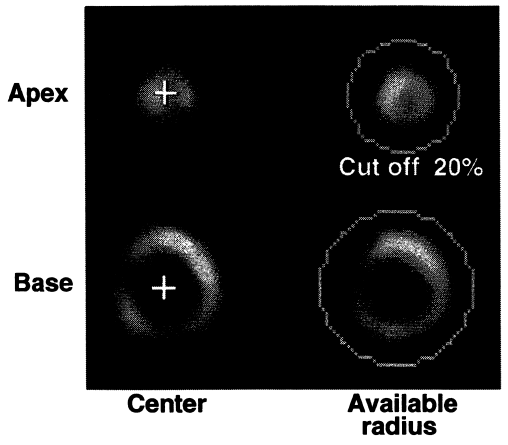

Fig. 5 The centers and the radii of the apical and the basal images at the end-diastole and the end-systole are determined by manual, whereas they at any frames are automatically determined by selecting 20% of the maximal count as the threshold level.

the basal images at the end-diastole and the end-systole were determined by manual. The portion of myocardium of the left ventricle was defined as the area whose counts are equal to 20% (threshold value) of the maximal myocardial counts. The centers and the radii on the apical and the basal images in the other slices were determined by Eq. 1 (Fig. 5). Each short-axis image was divided by 40 radii into 40 segments. Subsequently time-activity curve was generated from the total counts included in each segment plus both neighboring segments.

Curve fitting and calculation of parameters

Totally four hundred of time-activity curves from each segment were fitted to the second order invert fourier function. By analyzing fitted curves and these differential curves (Fig. 6), we estimated following parameters ; Max (End-systolic count), Min (End-diastolic count), CI (Count increase), %CI (Percent count increase), Uptake, PCR (Peak contraction rate), PDR (Peak distention rate) and CT (Contraction time), where are Max : maximal count on the fitted time activity curve, Min : minimal count

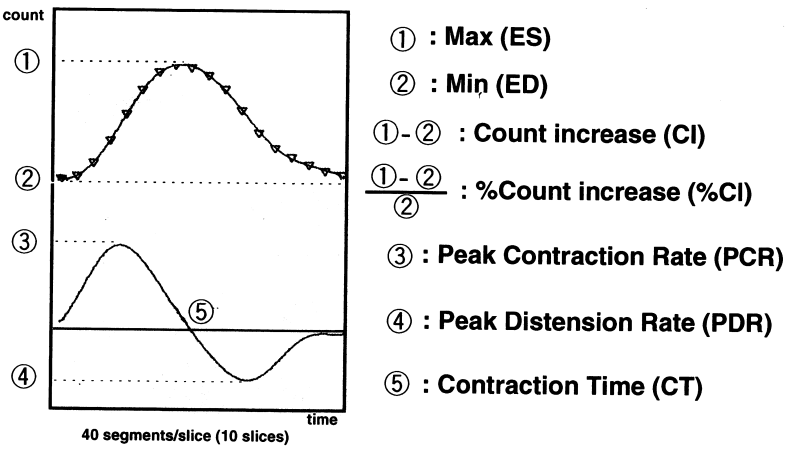

Fig. 6 A curve obtained by fitting the second order Fourier function to a time-activity curve, and its differential curve. Following parameters are derived from these curves ; Max (End-systolic count), Min (End-diastolic count), %CI (Percent count increase), Uptake, PCR (Peak contraction rate), PDR (Peak distention rate) and CT (Contraction time)

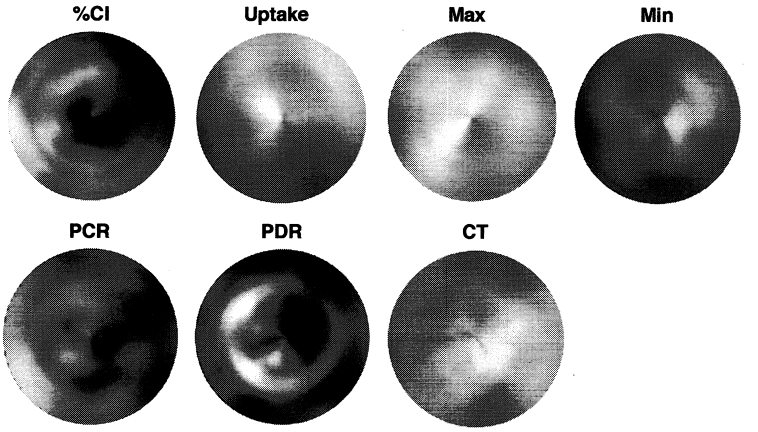

Fig. 7 Functional G-maps of %CI, %Uptake, %Max, %Min, %PCR, %PDR and %CT in a normal subject shows the difference among each segment respectively. Each scale except %CI is represented as 100%, normalized by the maximal value in every parameter, whereas %CI is represented as 100% at the delayed contraction time.

on the fitted time activity curve, CI : maximal count - minimal count (=amplitude × 2), %CI : (maximal count - minimal count) / minimal count, Uptake : average count in the fitted time activity curve, PCR : peak rate of count increasing in end-systolic phase, PDR : peak rate of count decreasing in end-diastolic phase, CT : interval from time zero to maximal count.

Assessment of new parameters

Each functional G-map was made of 10 slices from apex to base and divided into five regions : apex, anterior, septal, inferior, and lateral regions. Then the regional mean values were calculated. The percent Max (%Max), %Min and %Uptake were obtained by dividing Max, Min and Uptake by the maximal value of each parameter in five regions respectively. The percent CT (%CT) was obtained by dividing CT by the minimal value in five regions. The percent PCR (%PCR) and %PDR were obtained by dividing the PCR and PDR by each Min value in five regions respectively. Finally the functional G-maps were interpreted by visual analysis.

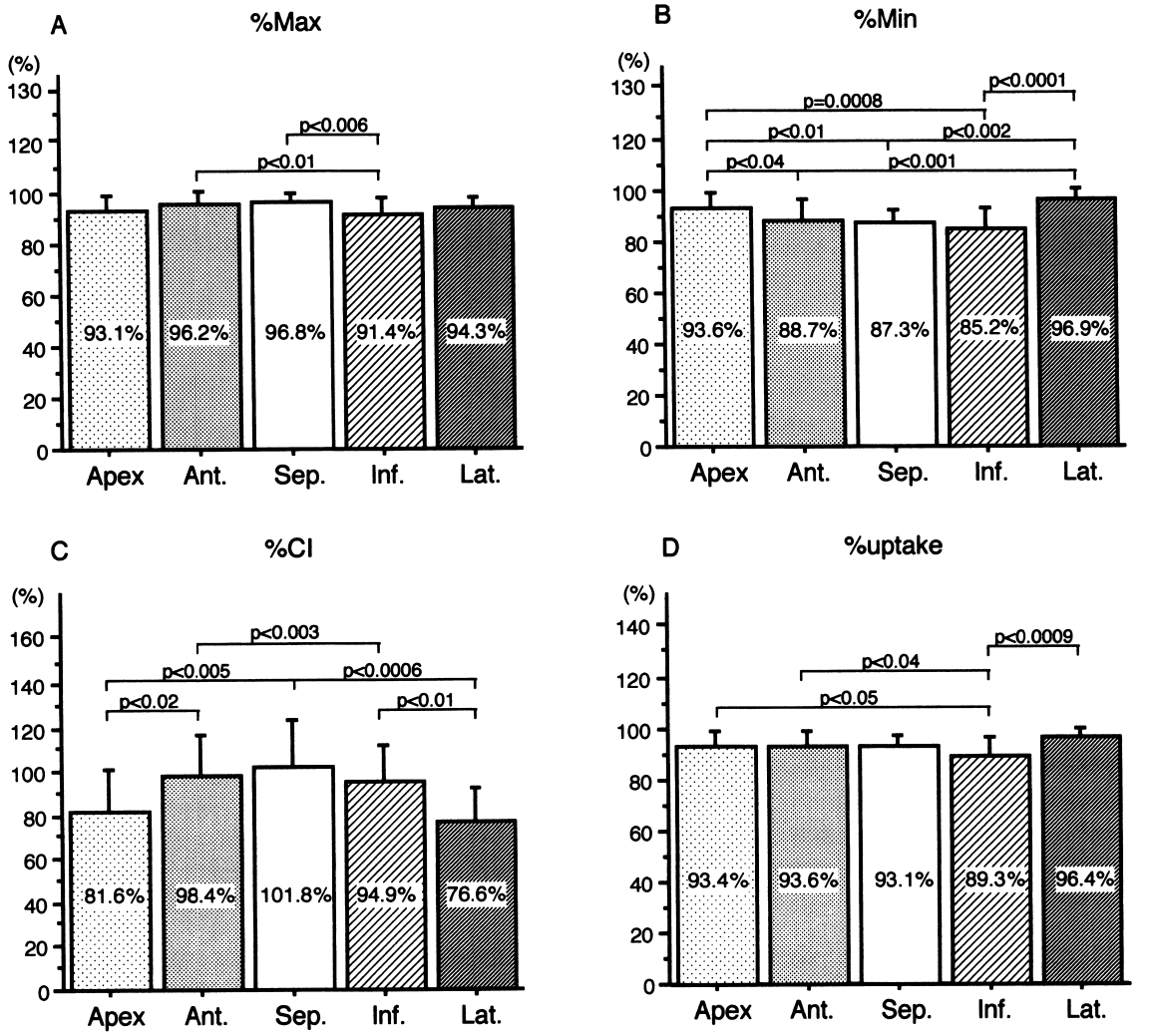

Fig. 8 Bar graphs showing mean ±lS.D. of each parameter in 14 normal subjects. A : %Max, B : %Min, C : %CI, D : %Uptake. Ant. : anterior, Sep. : septal, Inf. : inferior, Lat. : lateral

Statistical analysis

All results were expressed as mean ± lS.D. The significant difference was assessed with Fisher's Protected Least Significant Difference (Fisher's PLSD). Significance was defined at the level of $p<0.05$.

RESULTS

Figure 7 shows Functional G-maps depicted by each parameter in normal subject. Figure 8 and 9 show the means of each parameter in five regions. The %Max was greater in the anterior and septal regions, but lower in the inferior region. Comparing with the means of parameters among these regions, the value in the inferior region was significantly lower than that in the anterior and septal regions (91.4% vs 96.2%, $p<0.01$: 91.4% vs 96.8%, $p<0.006$) (Fig. 8-A). The %Min was greater in the apex (93.6%) and lateral regions (96.9%), whereas the %Min in the septal (87.3%) and inferior (85.2%) regions were significantly lower than those in the other regions (Fig. 8-B).

The means of %CI in five regions were 81.6% ±19.6% (apex), 98.4% ±18.0% (anterior), 101.8 %±21.5% (septal), 94.9% ±17.1% (inferior) and 76.6%±15.4% (lateral). The significant difference was more stronger between the septal and lateral regions ($p<0.0006$) (Fig. 8-C). The distribution of %Uptake was almost homogenous, but

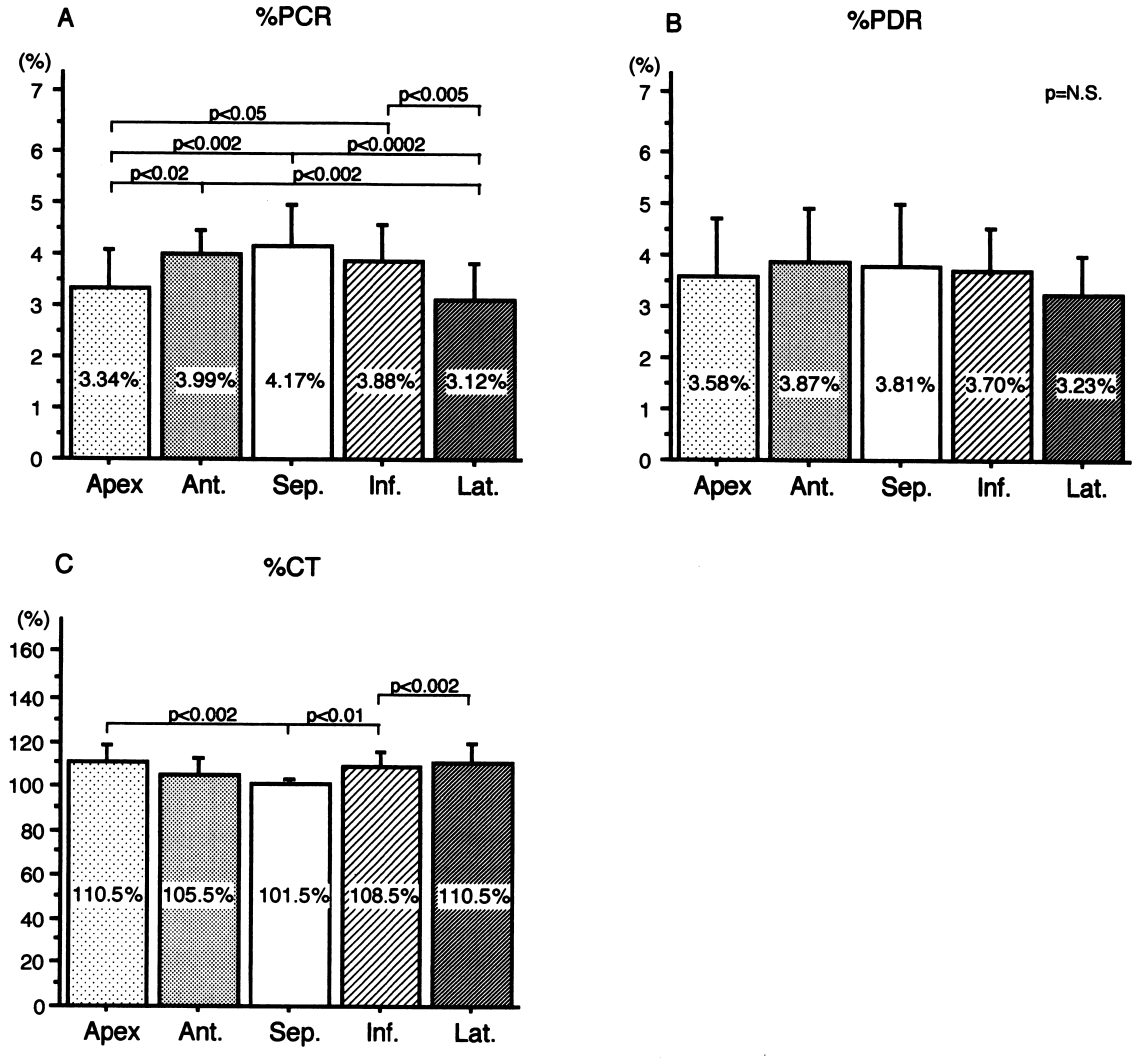

Fig. 9 Bar graphs showing mean ±1S.D. of each parameter in 14 normal subjects. A : %PCR, B : %PDR, C : %CT. Other abbreviations are shown in Fig. 8.

the %Uptake in the inferior region was significantly lower than that in the lateral region (89.3% vs 96.4%, $p<0.0009$) (Fig. 8-D).

The %PCR showed a tendency nearly similar with %CI and greater in the septal (4.17%), anterior (3.99%) and inferior regions (3.88%). The significant difference was more stronger between the septal and lateral regions ($p<0.0002$) (Fig. 9-A). On the other hand, %PDR in the apex (3.58%) and lateral (3.23%) regions were slightly lower than the values in the other regions, although significant difference was not shown among each region (Fig. 9-B).

The means of %CT was greater in the apex (110.5%), inferior (108.5%) and lateral regions (110.5%), and the value in the septal region (101.5%) was significantly lower than that in these regions ($p<0.002$) (Fig. 9-C).

DISCUSSION

Since ECG gated SPECT in cardiac blood pool scintigraphy was first reported by Moore et al.[6] in 1980, many kinds of parameters including LVEF, amplitude, phase, %CI and %WT were documented[7)-11)]. However only little authors reported the quantitative method using these parameters and visual analysis for the functional image[7)-8), 12)]. Therefore we tried new analysis (Functional G-maps) on ECG gated SPECT to assess PCR, PDR, and CT as well as

Max, Min, %CI, and %Uptake.

Main characteristic of Functional G-maps method is to allow improvement on the basis of the slice thickness correction and the calculation for time activity curve. Excluding the effect of different apex-base length in any frame during a cardiac cycle, we made 10 short-axis images with the same slice thickness for each frame. Time activity curve were calculated in each segment from the total counts included in each segment plus both neighboring segments. The generation of time activity curve in the old report was performed using the mean or the maximal counts[8)-9), 12)]. We used the total counts to generate time-activity curve and parameters of PCR, PDR and CT, therefore, could be detectable. The abilities of contraction and distension of the myocardium, which were estimated by means of ECG gated SPECT were not fully compared with that estimated by means of the other modality. Although further study is required, it seems that these parameters can be helpful on the clinical use.

It was found out that the center of short-axis images move along the long axis from the end-systole to the end-diastole and cavity size of the left ventricle is variable[10)], so that the center of the short-axis images must be instituted according to size of the left ventricular cavity. For our method, the centers of the apical and the basal images at the end-diastole and the end-systole were found out by manual, and the centers of the other slices were automatically determined using formula Eq. 1.

Tc-99m-myocardial imaging agents have characteristic of enhanced extracardiac activity. To reduce the influence from hepatic activity, the area of myocardium was determined using the threshold of 20% of the maximal myocardial counts after the effective radius of the myocardium was determined by manual.

Different %CI in different segments was shown in the normal cases. The %CI were greater in the septal (101.8%), anterior (98.4%) and inferior (94.9%) regions, whereas that in the apex (81.6%) or inferior (76.6%) regions was significantly lower than the other regions. Particularly, stronger significant difference was shown between the septal and lateral regions ($p<0.0006$). The value of our results were slightly higher than that reported by other authors. It was considered that the difference was caused by the difference of myocardial counts which was used for the generation of time activity curve. Shirakawa et al.[13)] and Mochizuki et al.[8)] used the mean and the maximal counts to generate time activity curve respectively. On the other hand, we used the total counts included in each regions plus both neighboring regions.

As before, the estimation for the myocardial systolic and diastolic abilities as the cardiac function has been presented the measurements of peak ejection rate (PER) and peak filling rate (PFR) — that is, the maximal up and down slopes of the left-ventricular volume curve, normalized to end-diastolic counts[14)]. This functional G-maps made it possible to assess the detailed cardiac function by using PCR, PDR and CT obtained from ECG gated SPECT.

In this study, the effect of rotation of the left ventricle was ignored. It is known that contraction of the obliquely oriented fibers results in a counterclockwise twist of the left ventricle on the long-axis[15)-16)]. Although the twist phenomenon is difficult to be corrected, it is required for more accurate analysis.

When a single-head rotating gamma camera was used, it took 27 minutes and 20 minutes in data acquisition and data processing, respectively. If we employ a multi-head rotating gamma camera, acquisition time would be drastically reduced.

In conclusion, we developed automatic program to calculate the values of parameters including Max, Min, %CI, Uptake, PCR, PDR, and CT and represented these values on the polar maps. The functional G-maps demonstrated clearly regional cardiac function. Therefore this method is expected to be helpful for accurate assessment of cardiac function.

ACKNOWLEDGMENTS

This paper was presented at the 35th Annual meeting of Japanese Society of Nuclear Medicine in Yokohama, on October 4, 1995.

REFERENCES

1. Canby, R.C. et al. : Relations of the myocardial imaging agents 99mTc-MIBI and 201-T1 to myocardial blood flow in a canine model of myocardial ischemic insult. Circulation, 81 : 289-296, 1990.
2. Glover, D.K. et al. : Myocardial kinetics of Tc-MIBI in canine myocardium after dipyridamole. Circulation, 81 : 628-636, 1990.
3. Sinusas, A.J. et al. : Technetium-99m-tetrofosmin to assess myocardial blood flow : experimental validation in an intact canine model of ischemia. J Nucl Med, 35 : 664-673, 1994.
4. Chua, T. et al. : Gated technetium-99m sestamibi for simultaneous asset of stress myocardial perfusion, postexercise regional ventricular function and myocardial viability. Correlation with echocardiography and rest thallium-201 scintigraphy. J Am Coll Cadiol, 23 : 1107-1114, 1994.
5. Kim, A.W. et al. : Comparison of Technetium-99m sestamibi-gated tomographic perfusion imaging with echocardiography and electrocardiograhy for determination of left ventricular mass. Am J Cardil, 77 : 750-755, 1996.
6. Moore, L.M. et al. : ECG-gated-emissions-computed tomography of the cardiac blood pool. Radiology, 134 : 233-235, 1980.
7. Gerhard, G. et al. : Reconstruction of fourier coefficients : a fast method to get polar amplitude and phase images of gated SPECT. J Nucl Med, 31 : 1856-1861, 1990.
8. Mochizuki, T. et al. : Assessment of systolic thickening with Thallium-201 ECG-gated single-photon emission computed tomography : A Parameter for local left ventricular function. J Nucl Med, 32 : 1496-1500, 1991.
9. David, C. et al. : Determining the accuracy of calculating systolic wall thickening using a fast fourier transform approximation : A Simulation study based on canine and patient data. J Nucl Med, 35 : 1185-1192, 1994.
10. Adachi, I. et al : Assessment of myocardial contraction and relaxation with 99m-Tc-tetrofosmin multigated myocardial SPECT. Kakuigaku, 31 : 1453-1463, 1994.
11. Toba, M. et al. : Evaluation of left ventricular diastolic function using gated SPECT with 99m-Tc-MIBI. Kakuigaku, 33 : 409-413, 1996.
12. Sugihara, H. et al. : Assessment of left ventricular count increase with ECG-gated 99m-Tc-MIBI SPECT using a shingle-head rotating gamma-camera. Kakuigaku, 31 : 1201-1208, 1994.
13. Shirakawa S. et al. : Assessment of left ventricular wall thickening with gated 99m-Tc-MIBI SPECT －value of normal file－. Kakuigaku, 32 : 643-650, 1995.
14. Bacharach, S.L. et al. : Left-ventricular peak ejection rate, filling rate, and ejection fraction : Frame rate requirements at rest and exercise. J Nucl Med, 20 : 189-193, 1978.
15. Buchalter, M.B. et al. : Noninvasive quantification on left ventricular rotational deformation in normal humans using magnetic resonance imaging myocardial tagging. Circulation, 81 : 1236-1244, 1990.
16. Yun, K.L. et al. : Alteration in left ventricular diastolic twist mechanics during acute human cardiac allograft rejection. Circulation, 83 : 962-973, 1991.

心電図心筋ゲートSPECTの新しい心機能解析法 (Functional G-maps)：正常人における検討

小野口昌久，丸野　廣大，高山　輝彦，村田　　啓

要　　旨

心電図ゲートSPECTを用いて心機能を正確に評価するために，新しい解析法(Functional G-maps)を試みた。Tc-99m-tetrofosmin 1110MBqの投与1時間後にゲートSPECTを撮像し，データを1心拍を12分割して収集した。SPECTの短軸像を最大収縮末期から最大拡張末期まで，スライス厚を補正して厚さの等しい10スライスの短軸像を再構築した。次に，各短軸像を40領域に分割し，領域内のトータルカウントを用いて時間放射能曲線を作成し，2次フーリエ級数で近似した。合計400本の曲線を自動解析して，収縮末期カウント（Max），拡張末期カウント（Min），カウント増加率（%CI），摂取率（Uptake）の他に，新たに最大収縮速度（PCR），最大拡張速度（PDR），駆出時間（CT）を算出し，これらを用いて機能画像の作成と指標値の算出を行った。正常例では%Maxは前壁(96.2%)から中隔（96.8%）にかけて値が高く，%Minは心尖部（93.6%）と側壁（96.9%）で高値を示した。%CIと%PCRはほぼ同様な傾向を示し，中隔（101.8%，4.17%），前壁(98.4%，3.99%)，下壁（94.9%，3.88%）では有意に高値を示した。一方，%PDRは心尖部（3.58%）や側壁（3.23%）では他の3領域に比べ有意差は認められないものの，低値を示した。CTは心尖部と側壁（110.5%）で高値を示した。今回，新しく作成したFunctional G-mapsは心筋血流の評価と同時に，心機能を種々の指標によって容易に定量化，かつ視覚化でき，臨床的に有用であると思われた。